SIMULATED AND MEASURED MAGNETIC PERFORMANCE OF A DOUBLE APPLE-II UNDULATOR AT THE CANDIAN LIGHT SOURCE

C. Baribeau, L.O. Dallin, J. Helfrich, T. Pedersen, M. Sigrist, W.A. Wurtz, Canadian Light Source, University of Saskatchewan, 44 Innovation Boulevard, Saskatoon, Saskatchewan, S7N 2V3, Canada

Abstract

Assembly and shimming are underway for a double APPLE-II type undulator (two magnet arrays installed side by side on a single support structure) at the Canadian Light Source. The device is planned to be installed in spring 2017. Extensive preparation was done prior to assembly, particularly in the development of a simulated annealing algorithm for magnet virtual shimming, as well as assembly procedures that minimized positional errors in the installed magnet blocks. In this paper we present measurements taken throughout shimming the first elliptically polarizing undulator (EPU), and compare with predictions from a RADIA [1] model where each magnet block was magnetized uniquely according to individual Helmholtz coil measurements.

DEVICE ASSEMBLY

The double APPLE-II consists of one high energy undulator (EPU55) and one low energy undulator (EPU180). The high energy device contains 70 × 55 mm periods, totaling 1148 magnet blocks with end sections; the low energy device contains 20 × 180 mm periods. Assembly of EPU55 began in summer 2015 and completed in 9 weeks, with an additional week to take measurement midway through assembly. Shimming and measurements of EPU55 were completed in full, concluding in spring 2016, before assembly of EPU180 began.

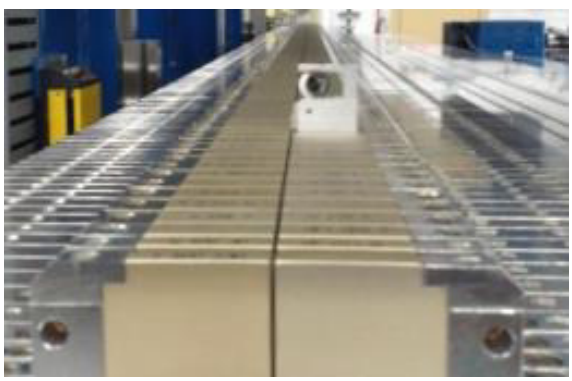

Figure 1: Reflector ball and jig on lower girder of EPU55 for laser tracker positioning.

During block installation, positioning of each magnet was measured using an API T3 laser tracker and a custom jig to mount a ½" ceramic reflector ball. The ball and jig are shown in Fig. 1. The layout of an individual magnet holder is shown in Fig. 2. Dowel pins (yellow) determine the holder's longitudinal position relative to the girder; vertical bolts (red) fasten the holder to the girder, while positioning bolts and set screws allow for fine adjustments of horizontal (green) and vertical (blue) position. Throughout installation, magnet positions were kept accurate to a reference position within 30 µm.

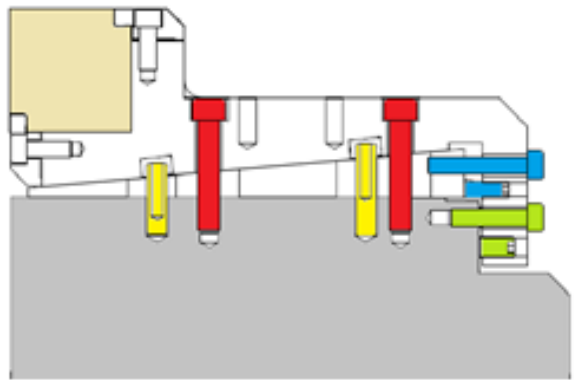

Figure 2: Magnet block, holder, and girder assembly.

DEVICE PERFORMANCE

Initial Measurements & Simulation

Prior to shimming, EPU55 had a large dipole component in the vertical field integrals, shown in Table 1. The large initial integrals are a result of a mistake made at the magnet block sorting stage, where the horizontally polarized magnets (which have 90° symmetry) were installed in the opposite orientation relative to what the block sorting code intended. Field integral measurements are shown in Fig. 3 alongside values calculated from a RADIA model of EPU55, using the as-built magnet sort list. The vertical component agrees well in magnitude, but the structure differs between measurement and simulation, which may be a result of systematic errors in the magnet block Helmholtz coil measurements.

Table 1: Initial EPU55 Parameters at 15.5 mm Gap

Parameter	Planar Mode	Vertical Mode
On-Axis IBx (G·cm)	-71	-51
On-Axis IBz (G·cm)	536	500
On-Axis IIBx (G·cm^2)	-54,000	-49,000
On-Axis IIBz (G·cm^2)	160,000	157,000
RMS Phase Error (°)	9.64	14.4

ISBN 978-3-95450-147-2

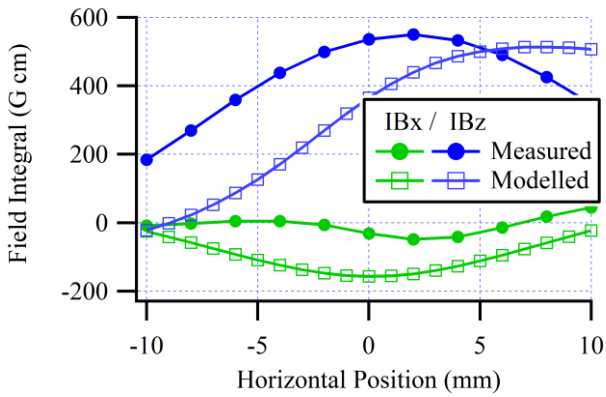

Figure 3: Measured and simulated transverse field integrals for EPU55 at 15.5 mm gap and planar mode prior to device shimming.

Virtual Shimming with the Simulated Annealing Algorithm

An implementation of the simulated annealing algorithm (SA) [2] was developed at CLS using Mathematica. The SA algorithm is used at multiple stages of EPU assembly and shimming, including magnet block sorting, virtual shimming, and magic finger shimming. The SA algorithm has been used successfully for shimming two previous EPUs at the CLS [3], however, the code underwent extensive upgrades for the QMSC double EPU. This was in part necessary due to sweeping hardware upgrades to the CLS magnet measurement lab, but the opportunity was also taken to write a suite of new, more effective cost functions, to better drive the SA algorithm's optimization.

At each shimming iteration, detailed measurements of the magnetic field and 1st and 2nd field integrals were taken using a 3D SENIS Hall probe and a BeCu flipping coil, respectively. The standard measurement set included five modes spanning three polarizations – planar, vertical, and quarter-phase elliptical – at gaps from 15.5-25 mm. Later on, as limit switch and encoder offsets were finalized, we were able to extend the minimum gap in the magnet lab to 14.5 mm.

To determine the next iteration of virtual shims, measurements from the most recent iteration are passed into the SA algorithm. Measurements are modified by shim signatures, i.e. the predicted local change in field (integral) due to displacing a magnet block of a given polarization by a discrete distance (e.g. 50 µm). Shim signatures are calculated from a RADIA model of the EPU for each gap and polarization mode under consideration.

Using the modified field and field integrals, the SA algorithm calculates derived parameters such as: extrema in 1st field integrals; exit beam trajectories; RMS of phase error; trajectory straightness; and magnetic field taper. These parameter costs are the metrics by which the SA algorithm judges new shim arrangements. Over the course of several hours, a typical run of the algorithm evaluates >30,000 configurations, and ultimately returns the shim set that most improves the considered parameters.

Intermediate Measurements

EPU55 was shimmed over 34 iterations, including 5 small iterations used for testing the SA algorithm. Of the non-test iterations, 24 were virtual shimming, which ranged from 15-40 shims per iteration. The installation of small "magic finger" end magnets was performed over five iterations.

The evolution of selected parameters throughout the shimming process are shown below for EPU55. Exit beam trajectories are shown in Fig. 4, normal multipole components in Fig. 5, and skew multipole components in Fig. 6. Note the break between iterations 25 and 26, where the measured gap was lowered from 15.5 to 14.5 mm, and the vertical axes zoomed.

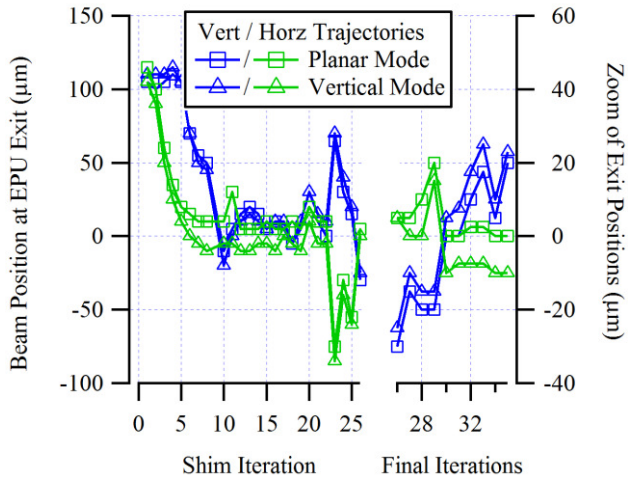

Figure 4: Improvements to exit trajectory in planar and vertical modes over course of shimming.

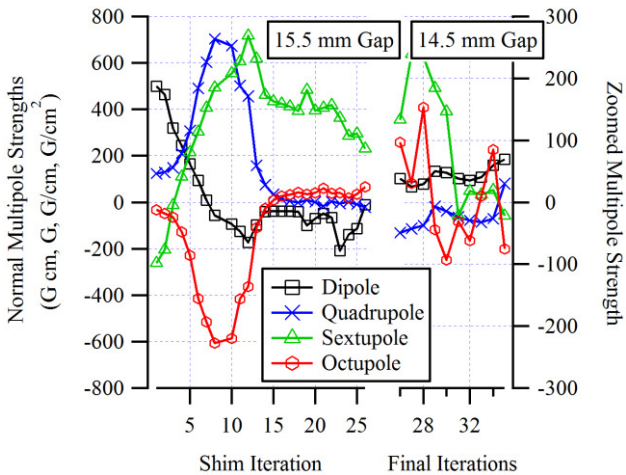

Figure 5: Improvements to normal multipole components over course of shimming.

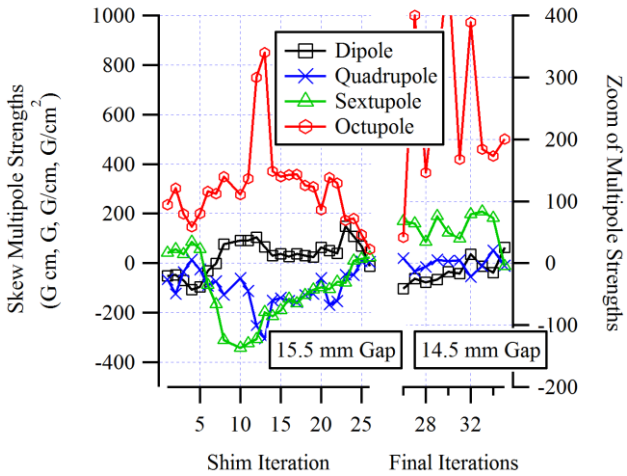

Figure 6: Improvements to skew multipole components over course of shimming.

Final Measurements & Simulation

Upon completion of shimming, EPU55's measured field characteristics met design specifications for the target photon energy range (200-1000 eV), with few exceptions. There remains a strong on-axis 2nd field integral, varying over the gap range on the order of 20,000 G·cm^2; however, it is straightforward to mitigate using correction coils, which will be installed in the straight section. The phase error in planar mode and 1st field integral parameters are well behaved at the minimum photon energy (see Table 2). In fact, for planar polarization mode many parameters continue to remain within design specifications down to 125 eV (at 14.5 mm gap), well below the specified 200 eV low energy cutoff. The 10° phase error in circular mode is not of particular concern, as only the first harmonic will be used.

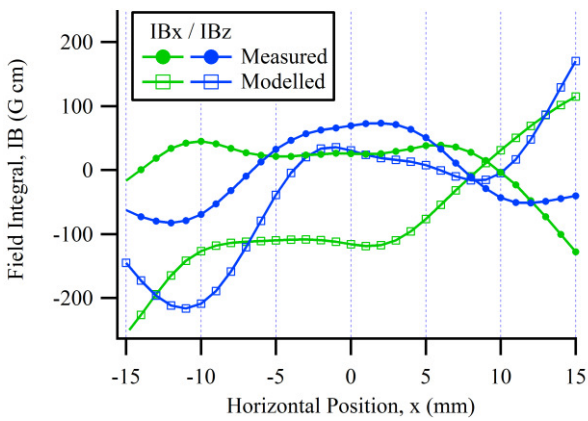

Figure 7: Measured and simulated transverse field integrals for EPU55 at 14.5 mm gap and planar mode after device shimming.

Field integral measurements are shown in Fig. 7 alongside values calculated from a RADIA model, which incorporates the magnet sort list, cumulative shims, and magic finger end magnets. There is qualitative agreement in the normal component; the modelled skew component, however, has a 32.5 G quadrupole component (i.e. slope) subtracted out, and there still remains a DC offset on the order of 200 G·cm. The model does not capture inhomogeneity errors in the magnets, nor does it account for potential systematic errors in the Hall probe or flip coil measurement systems, all of which may contribute to disagreement with measurement.

Table 2: Final EPU55 Parameters, 200 eV Photon Energy

Parameter	Design Limit	Measurement (Planar, Circular)
RMS Phase Error	6°	(4.43, 10.0)
Exit Bx 2nd Integral	5,000 G·cm^2	(18,000, 23,000)
Exit Bz 2nd Integral	5,000 G·cm^2	(5,900, 1,300)
Normal Dipole	50 G·cm	(49, 21)
Skew Dipole	50 G·cm	(21, 37)
N. Quadrupole	50 G	(18, 28)
S. Quadrupole	50 G	(-4.5, -4.7)
N. Sextupole	100 G·cm^{-1}	(-92, 42)
S. Sextupole	100 G·cm^{-1}	(-3, -12)
N. Octupole	150 G·cm^{-2}	(-25, -40)
S. Octupole	150 G·cm^{-2}	(-17, 143)

CONCLUDING OBSERVATIONS

Assembly and shimming of EPU55 is complete, with measurements of the device throughout the shimming process showing reasonable agreement with the undulator's RADIA model. Results indicate the SA algorithm is an accurate and effective tool for optimizing the EPU's field characteristics. With SA tuned and operational, shimming future EPUs at CLS is expected to take considerably less time.

REFERENCES

[1] P. Elleaume, O. Chubar and J. Chavanne, "Computing 3D magnetic fields from insertion devices", PAC97 (1997).

[2] S. Kirkpatrick, C. D. Gelatt, M. P. Vecchi, "Optimization by Simulated Annealing", Science New Series, Vol. 220 (1983) 671-680.

[3] L. Dallin, M. J. Sigrist, T. Summers, "Canadian Light Source Update", EPAC (2006).

ISBN 978-3-95450-147-2